# Optimization of a Muon Collider Interaction Region with Respect to Detector Backgrounds and the Heat Load to the Cryogenic Systems\*

C. J. Johnstone and N. V. Mokhov

Fermi National Accelerator Laboratory, P.O. Box 500, Batavia, Illinois 60510, U. S. A.

#### **ABSTRACT**

In a  $2 \times 2 \, \text{TeV} \ \mu^+ \mu^-$  Collider almost 15 MW of power is deposited in the machine and detector components due to the unavoidable  $\mu \to e \nu \tilde{\nu}$  decays. The resulting heat load to the cryogenic sytems and the background levels in the collider detectors significantly exceed those in any existing or designed hadron and  $e^+e^-$  colliders. This paper shows that by carefully designing the final focus system, by embedding shielding and by taking other protective measures the heat load and backgrounds can be mitigated by several orders of magnitude.

#### I. INTRODUCTION

Increasing interest in a high-energy high-luminosity  $\mu^+\mu^-$  collider project [1, 2] is based on the physics potential of such a machine which is beyond or complementary to what can be accomplished at  $e^+e^-$  and hadron colliders. There remain many issues to be examined in such a machine, especially technical ones. One of the most serious technical problems in the design of a muon collider arises from muon decay. With  $2 \times 10^{12}$  muons in a 2-TeV bunch, there are  $2 \times 10^5 \ \mu \rightarrow e \nu \tilde{\nu}$  decays per meter in a single pass through an interaction region (IR), or  $6 \times 10^9$  decays per meter per second. Both the decay electrons (with an energy of about 700 GeV) and the synchrotron photons emitted by these electrons in a strong magnetic field induce electromagnetic showers in the collider and detector components. Almost 15 MW of power is deposited in the storage ring, which is about 2kW every meter. The resulting heat load to the cryogenic systems and the background levels in the collider detectors exceed the past operational experience and even the upgrade designs at hadron and  $e^+e^-$  colliders. Substantial suppression of the induced background levels is critical in the concept of a muon collider and detector [3, 4, 5]. The design of a storage ring and, in particular, an IR in such an environment is a difficult and challenging problem. The merits of different approaches to solving beam-induced energy deposition issues in a muon collider IR are the subject of this paper. Calculations of the particle interactions in the lattice and detector components for a 2 TeV muon beam are performed with the MARS code [6].

## II. MUON-DECAY ENERGY DEPOSITION

The unacceptable level of energy deposition in the superconductoring (SC) elements of the ring impacts not only the technical implementation of SC magnets, but also influences the design of the lattice itself.

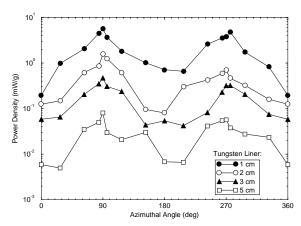


Figure 1: Azimuthal distribution of power density in the first SC cable shell in the collider arc for different tungsten liners inside the aperture for one 2 TeV muon beam.

Two solutions to the beam-induced heating problem have been suggested for the muon collider arcs and the IR. The first involved surrounding the vacuum chamber with a thick absorber which increases significantly the bore of the SC magnets [2, 4]. Fig. 1 shows the azimuthal dependence of power deposited in the first cable shell of the arc dipoles for tungsten liners with varying thicknesses. In the arc there is a strong azimuthal dependence of power density which exceeds the expected quench limits of SC magnets by more than an order of magnitude. Fig. 2 shows the power dissipation per meter as a function of liner thickness in the various cold components of a magnet: the liner, liquid helium,

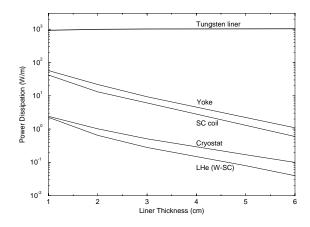


Figure 2: Power dissipation in the arc magnet components *vs* tungsten liner thickness for one 2 TeV muon beam.

 $<sup>^*</sup>$  Work supported by the Universities Research Association, Inc., under contract DE-AC02-76CH00300 with the U. S. Department of Energy

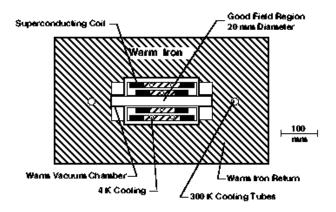


Figure 3: 8.5 T dipole with warm iron and SC coils moved off the mid-plane.

SC coils, yoke, and cryostat. From this figure it is clear that at least 6 cm of tungsten is required to shield arc dipoles with cosine theta SC coils.

A second approach, based on the specific azimuthal distribution of power dissipation in the arc magnets (Fig. 1), entails a design with cold or warm iron and the SC coils completely separated and removed from the mid-plane [2] as shown in Fig. 3.

#### III. IR DESIGN PROBLEMS

The MARS studies have shown that the two quadrupoles nearest the interaction point (IP) also require a minimum of 6 cm of tungsten. Even with a relaxed  $\beta^* = 3$  cm IR lattice [7] a power dissipation in these quadrupoles range from 4 to 13 kW. An acceptable level is about 10 W/m so these values are too high by two orders of magnitude. Furthermore, the energy deposition is much more uniform and does not exhibit the azimuthal behavior found in the arc. Therefore, the second solution, a noncosine theta magnet, does not work for the SC IR quadrupoles.

In the IR adding a 6-cm liner increases the difficulty of an already problematic design, since the nonlinear attributes of the IR are strongly correlated with the strength of the final-focus quadrupoles [8]. The beam size at the quadrupole nearest the IP is only 2 cm; therefore, adding 6 cm to the aperture represents a factor of 4 decrease in the quadrupole gradient. The  $\beta$ -functions in the high-beta quadrupoles increase by roughly this factor, feeding an iterative effect: apertures increase further and gradients decrease correspondingly. This increase is over and above that attributable to the liner thickness alone. The chromaticities and nonlinearities associated with higher peak  $\beta$ -functions rise dramatically. The strength-times-length factor due to the high- $\beta$  quadrupoles remains essentially the same, at least in first order.

Since first-order chromaticity has approximately a linear dependence on the peak  $\beta$ -functions, it increases proportional to the gradient reduction. Higher orders of chromaticity, however, display a stronger dependence – an increase of about two orders of magnitude for a factor of two decrease in gradient. Therefore the net effect of a thick liner is to increase dramatically the nonlinear behavior of the IR.

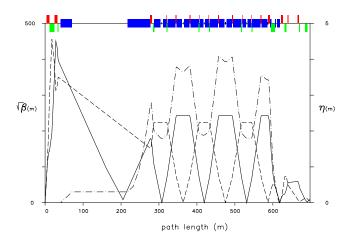


Figure 4: Horizontal (solid line) and vertical (dashed line)  $\beta$ -functions in the  $\beta^* = 3$  mm IR lattice. Dot-dashed line shows the dispersion.

## IV. REDUCTION OF HEAT LOAD

Tables I,II,III show the evolution of the IR design for a 2-TeV  $\mu^+\mu^-$  collider in terms of total power dissipated in the SC quadrupoles, liners, and, in the final table, the tungsten collimators and sweep dipoles. In the tables quadrupoles are denoted by Q, dipoles with D, and tungsten collimators in the drifts by DR-W. Power is in units of Watts per meter.

Table I: Power dissipation (W/m) in the  $4\sigma$  IR components.  $\beta^* = 3 \text{ mm } 270 \text{ m}$  lattice with a 3-cm tungsten liner inside the SC magnets (May 1996).

Element	QF51	QF52	DR-1	QD61	QD62	QF61	QF62	QD7	QF7
L(m)	5	1.455	0.25	7.49	7.49	6.06	6.06	4.29	7.35
Absorber	3522	13509	1979	2947	978	546	319	268	1858
Magnet	177	2154	-	24	10.3	5.4	4.6	2.7	18.3

Table II: Power dissipation (W/m) in the  $4\sigma$  IR components.  $\beta^* = 3 \text{ mm } 150 \text{ m}$  lattice with a 3-cm tungsten liner inside the SC magnets (July 1996).

Element	QF2	DR-1	QF51	QF52	QD6	QF6
L (m)	2	0.25	2	0.8	4.47	6.52
Absorber	3119	616	553	984	1724	293
Magnet	32	-	5.4	104	164	2.6

Compared to the early IR design with  $\beta^* = 3$  cm, the situation is much worse for a similar IR design with  $\beta^* = 3$  mm and 3 cm of protective tungsten liner (Table I). The power dissipation reaches high levels which are thousands of Watts per meter in one quadrupole (QF52). The more recent de-

Table III: Power dissipation (W/m) in the  $5\sigma$  IR components.  $\beta^* = 3$  mm 150 m lattice with a 2-cm tungsten liner inside the SC magnets,  $4\sigma$  tungsten collimators, four 8.5 T sweep dipoles (August 1996).

Element	QFP2	DR-W	QFS5-1	QFS5-2	DR-W	QDS6	DR-W	QFS6	D1H	D2V	QDS7
L (m)	2	0.15	2	0.8	0.15	4.47	0.15	6.52	15	15	1.08
Absorber	84.2	7488	34.4	144	25229	129	53338	824	1676	1100	253
Magnet	3.30	-	1.02	3.87	-	5.42	-	22.3	39	28	13

sign of Table II (July 1996), which employed strong nonsuperconducting quadrupoles near the IP (Bitter quadrupoles), reduced the peak  $\beta$ -function values and distributed the energy more evenly through the IR. The power levels, however, were still unacceptable in two of the SC quadrupoles: over a hundred Watts per meter.

Recent work is based on the lattice shown in Fig. 4. The basic approach is to spread decay electrons (positrons) along the entire final focus region instead of allowing them to hit apertures in the immediate vicinity of the IP (compare Fig. 5 and Fig. 6). By using dipoles upstream of the IR quadrupoles to sweep background particles, and by longitudinal shielding (tungsten collimators placed between elements), this approach has been successful in reducing the required liner thickness to 2 cm. To be effective, the sweep dipoles had to be 15 m long and superconducting with a poletip field of 8.5 T. Additionally, they had to be placed at least 1 m upstream of the elements to be protected. The sweep dipoles removed backgrounds propagating from the long drift preceding the high- $\beta$  quadrupoles and from the arcs. In the Table III a vertical sweep dipole is followed by a horizontal one. However, the effect on backgrounds is the same if both dipoles bend in the same plane. In the latest design, a pair of reversed, horizontally-bending dipoles were used in order to restrain the dispersion function through the long IR drift. Otherwise, the dispersion would reach an enormous value at the end of the 150 m drift, which is the beginning of the chromatic correction module.

In spite of the added dipoles, the heat load remained too high in most of the IR quadrupoles, in particular, the focussing and defocussing pair nearest the IP. Optically, these quadrupoles are the most significant in determining the nonlinear properties of the IR. To protect the inner IR quadrupoles, tungsten collimators were sandwiched between all quadrupoles. Calculations indicate the collimators should be 15 cm long, with a  $4\sigma$  aperture in order to fully shadow the SC quadrupoles which have a  $5\sigma$ aperture. As shown in Table III the combined effect of adding dipoles and collimators to the IR allowed the protective tungsten liner of the SC quadrupoles to be reduced to 2 cm. With the thinner liner the strength reduction of the IR quadrupoles is a factor of 2 compared to the case with no liner, but it is twice as strong as the case with a 6-cm liner. The smaller liner reduced peak  $\beta$ functions by about factor of two (from 400 to 200 km), and firstorder chromaticities were correspondingly halved (from -6000 to -3000 in the vertical plane, for example). Second and third order chromaticities fell by almost two orders of magnitude.

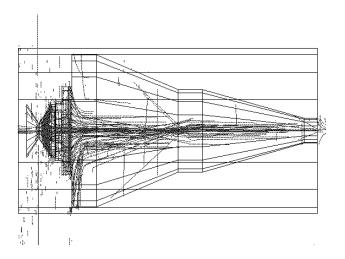


Figure 5: Positron tracks in the aperture of the  $\beta^*=3$  mm IR lattice (Fig. 4) for hundred 2-TeV  $\mu^+$  decays distributed uniformly in the 150-m IR. No sweep dipoles in the lattice. Aperture scale: 10 cm radially and 150 m longitudinally.

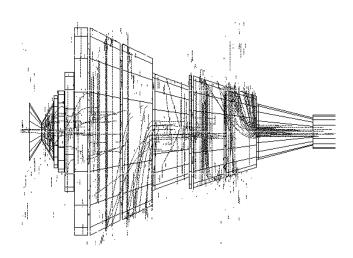


Figure 6: Positron tracks in the aperture of the  $\beta^*=3$  mm IR lattice (Fig. 4) for hundred 2-TeV  $\mu^+$  decays distributed uniformly in the 150-m IR. Four 8.5 T sweep dipoles are in the lattice. Aperture scale: 10 cm radially and 150 m longitudinally.

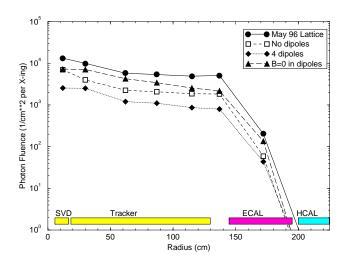


Figure 7: Radial dependence of photon fluence in the  $\pm 1.2$  m central detector region around the IP per  $2 \times 2$  TeV  $\mu^+\mu^-$  bunch crossing for different IR scenarios due to muon beam decays.

# 10<sup>5</sup> 10<sup>4</sup> Particle Fluence (1/cm\*\*2 per X-ing) 10 10<sup>2</sup> 10 10° 10 10-10 10 50 100 150 200 Radius (cm)

Figure 8: Radial dependence of particle fluence in the  $\pm 1.2$  m central detector region around the IP per  $2 \times 2$  TeV  $\mu^+\mu^-$  bunch crossing for the best IR configuration considered.

## V. BACKGROUND REDUCTION

A careful design of the final focus system with tapered liner apertures, sweep dipole magnets, interspersed tungsten collimators and additional tungsten collimators inside the detector with the aspect of two nozzles around the IP can reduce the background levels by several orders of magnitude. Fig. 7 shows the outcome of evenly distributing the decay electrons along the final focus region and the corresponding reduction in photon flux in the detector for the most recent IR designs. The best IR configuration reduces the background fluxes by a factor of 10. Even so, there still remains fluxes of a few thousand photons and neutrons and a few tens of charged particles (mainly  $e^{\pm}$ ,  $\pi^{\pm}$  and  $\mu^{\pm}$ ) per cm<sup>2</sup> of inner tracker per each bunch crossing (every 20  $\mu$ sec) (see Fig. 8). More work is obviously needed in the the design of the shielding measures in the immediate vicinity of the detectors.

# VI. SUMMARY

The combination of  $5\sigma$  aperture sweep dipoles and  $4\sigma$  aperture tungsten collimators reduced not only the heat load in the SC IR elements to acceptable values, but also improved tremendously the performance of the muon collider IR through strengthed quadrupole gradients. The reduction of dissipated power is almost a factor of 2000 in some elements for the same IR design. Operationally, therefore, the beam-induced energy deposition problems in the IR appear to be resolved (if the liners and collimators are kept at room or nitrogen temperature) and the remaining issues appear to be optical in nature. The results presented are only for beam entering the IR. Separate calculations for exiting beam indicate that it contributes to heat load in the distant ring components, starting about 130 m from the IP, but not in the IR quadrupoles. These magnets are shadowed by the collimators or protected by sweep dipoles. The backgrounds in the detector with the new IR, although reduced by a factor of 10, still require further work.

## VII. REFERENCES

- [1] 'Physics Potential and Development of  $\mu^+\mu^-$  Colliders', Sausalito-94, ed. by D. Cline, AIP Conference Proceedings **352** (1996).
- [2] ' $\mu^+\mu^-$  Collider: A Feasibility Study', The  $\mu^+\mu^-$  Collider Collaboration, BNL–52503; Fermilab–Conf–96/092; LBNL–38946 (1996).
- [3] G. W. Foster and N. V. Mokhov, 'Backgrounds and Detector Performance at a  $2 \times 2$  TeV  $\mu^+\mu^-$  Collider', in [1] pp. 178–190; also Fermilab–Conf–95/037 (1995).
- [4] N. V. Mokhov and S. I. Striganov, 'Simulation of Backgrounds in Detectors and Energy Deposition in Superconducting Magnets at μ<sup>+</sup>μ<sup>-</sup> Colliders', in AIP Conference Proceedings 372 of the 9th Advanced ICFA Beam Dynamics Workshop: Beam Dynamics and Technology Issues for μ<sup>+</sup>μ<sup>-</sup> Colliders, Montauk, NY, October 15–20, 1995, pp. 234-256; also Fermilab–Conf–96/011 (1996).
- [5] N. V. Mokhov, 'Comparison of Backgrounds in Detectors for LHC, NLC and μ<sup>+</sup> μ<sup>-</sup> Colliders', in *Proceedings of Symposium* on *Physics Potential and Development of* μ<sup>+</sup> μ<sup>-</sup> Colliders, San Francisco, CA, December 1995; Fermilab-Conf-96/062 (1996).
- [6] N. V. Mokhov, 'The MARS Code System User's Guide, Version 13(95)', Fermilab–FN–628 (1995).
- [7] C. J. Johnstone, K.-Y. Ng and D. Trbojevic 'Interaction Regions with Increased Low-Betas for a 2-TeV Muon Collider', in *AIP Conference Proceedings 372 of the 9th Advanced ICFA Beam Dynamics Workshop: Beam Dynamics and Technology Issues for*  $\mu^+\mu^-$  *Colliders*, Montauk, NY, October 15–20, 1995, pp. 178-189.
- [8] 'Zeroth-Order Design Report for the Next Linear Collider', The NLC Design Group, LBNL-5424; SLAC-474; UCRL-ID-124161; UC-414, May, 1996. C. Johnstone and A. Garren, 'An Interaction Region and Chromatic Correction Design for a 2-TeV Muon Collider', to appear in the Proceedings of the Snowmass Workshop, June-July, 1996.